Supporting Information

25S-Adamantyl-23-yne-26,27-dinor-1α,25-dihydroxyvitamin D_3: Synthesis, Tissue Selective Biological Activities and X-ray Crystal Structural Analysis of Its Vitamin D Receptor Complex

Rocio Otero, Michiyasu Ishizawa, Nobutaka Numoto, Teikichi Ikura, Nobutoshi Ito, Hiroaki Tokiwa, Antonio Mourino, Makoto Makishima, and Sachiko Yamada

A table of contents

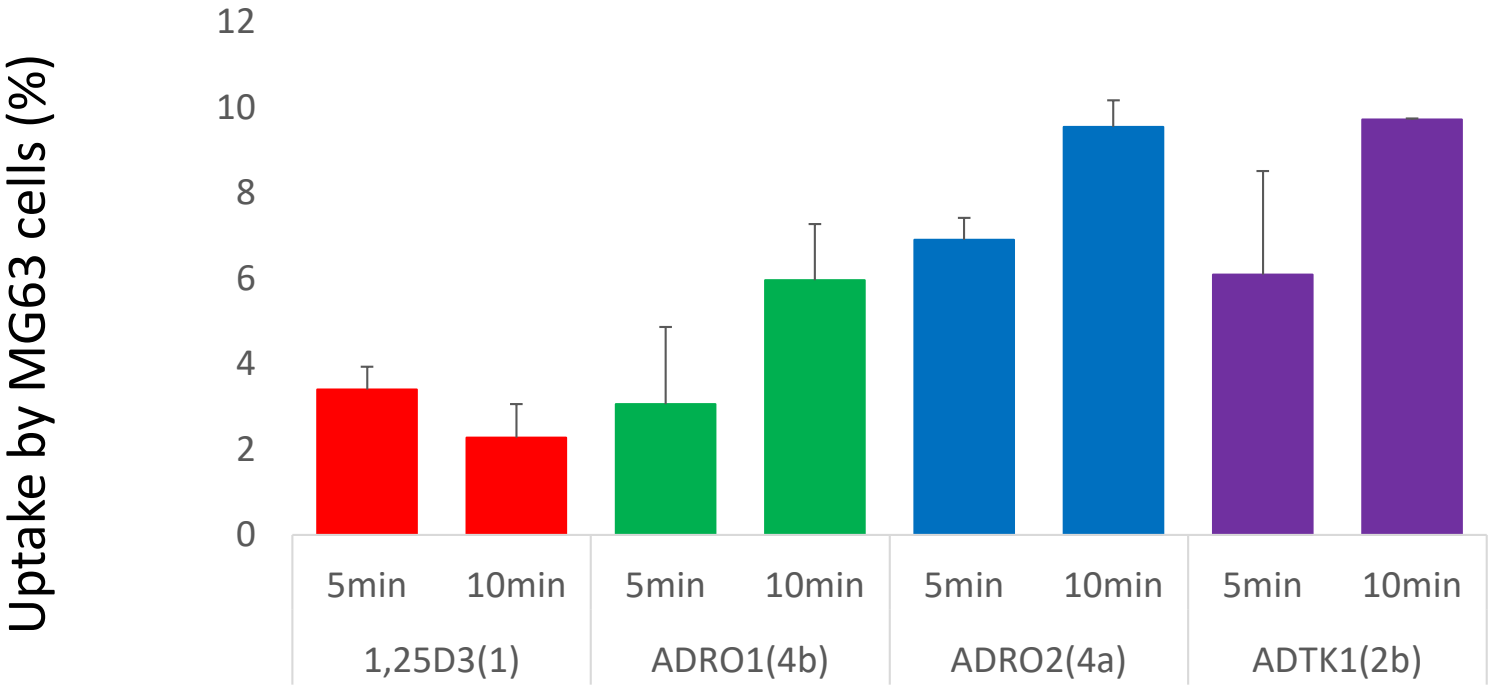

Figure S1A. Uptake of 1,25$(OH)_2D_3$ (**1**), ADRO1 (**4b**), ADRO2 (**4a**) and ADTK1 (**2b**) by MG63 cells.

MG63 cells plated in 35-mm dish at a density 2×10^5 cells/well (2.5×10^4 cells/cm^2) were incubated with 1 µM of each compound for 5 min or 10 min. The cells and medium were extracted separately by chloroform/methanol (3:1, v/v) . The extracts were analyzed by HPLC: Column, InertSustain C18 (5 µm; 4.6 mm × 250 mm) (GL Sciences Inc., Tokyo, Japan) ; mobile phase, linear gradient of 20–100% acetonitrile/water; UV detection, 265 nm for 1,25$(OH)_2D_3$ (**1**), ADRO1 (**4b**), ADRO2 (**4a**) and 250 nm for ADTK1 (**2**b). All values represent the means and error bars are standard deviations derived from triplicate assays.

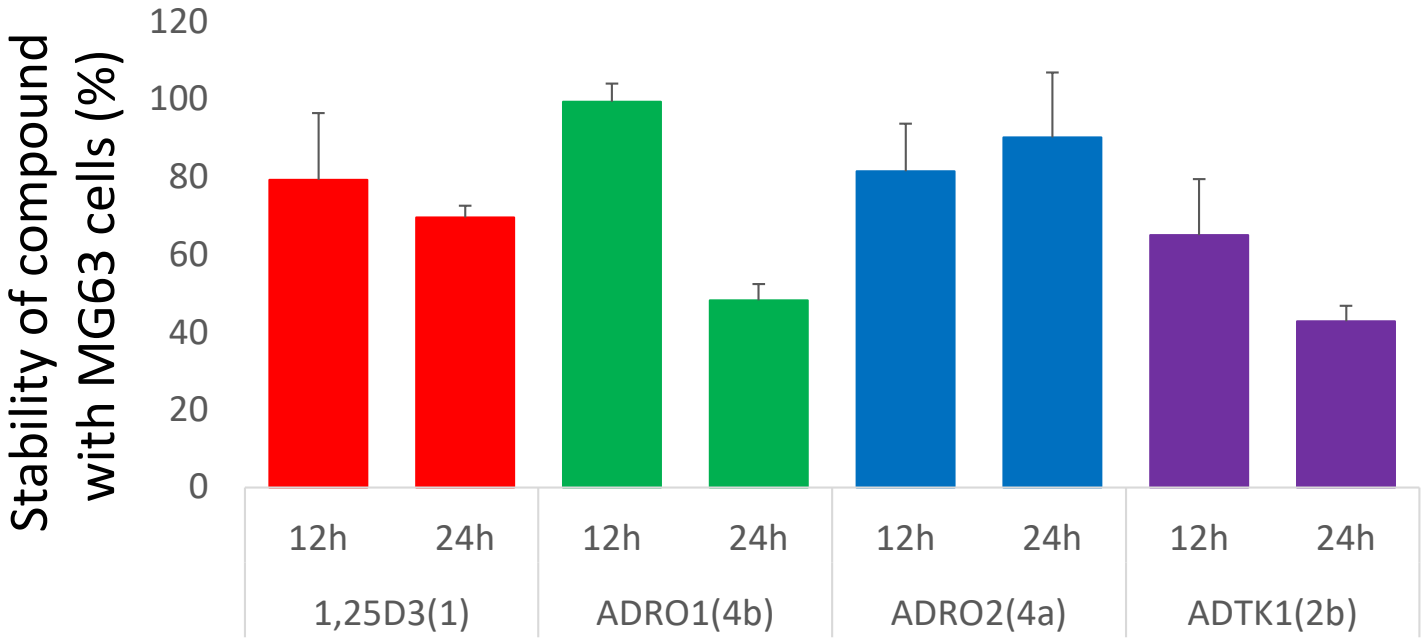

Figure S1B. Stability of 1,25$(OH)_2D_3$ (**1**), ADRO1 (**4b**), ADRO2(4a) and ADTK1 (**2b**) in MG63 cells. 1µM of 1,25$(OH)_2D_3$ (**1**), ADRO1 (**4b**), ADRO2 (**4a**) and ADTK1 (**2b**) were incubated with MG63 cells or without cells for 12h or 24h. Cell culture conditions were the same as those described in Figure S1. The percentage was calculated using a ratio of a value with cells to a value without cells. Each experimental mixture was extracted with chloroform/methanol (3:1, v/v). The extract was analyzed by HPLC (conditions are the same as those described in Figure S1). All values represent the means and error bars are standard deviations derived from triplicate assays.

Figure S2. Overall crystal structures of ternary rVDR-LBD/25*R*-isomer (**4a)** /DRIP205 co-activator complex. The protein and peptide are drawn by ribbon structures with rainbow colors (blue to red). The ligand **4a** is shown in a stick model with atom-type colors.

Figure S3. Van der Waals interactions (<4 Å, magenta lines) of **4a** (atom-type colors with green carbon) with VDR residues (atom-type colors). Fifteen VDR residues are interacting with the ligand **4a**.

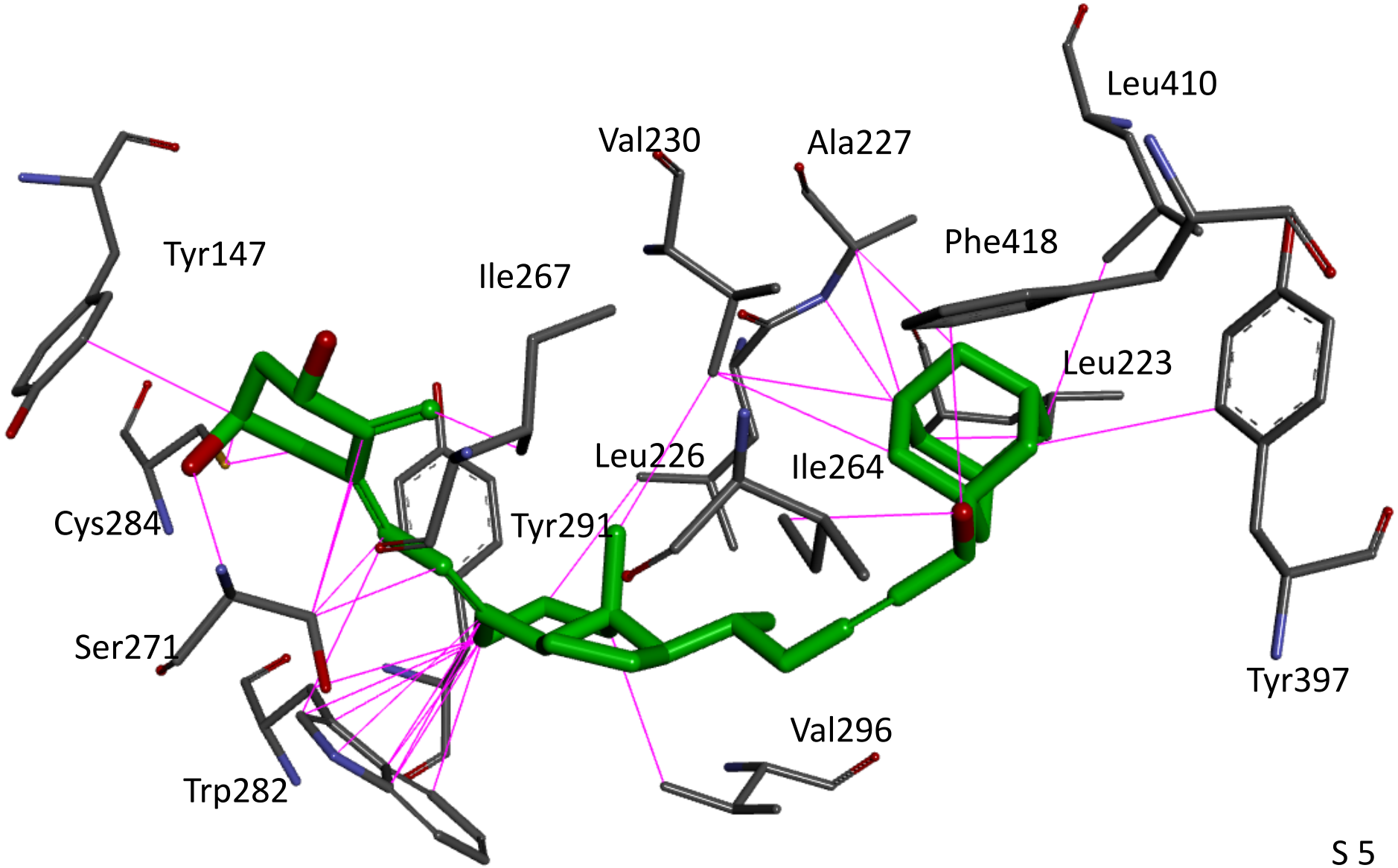

Figure S4. Electron density maps at the helix 11 region of VDR/ligand complexes. (A) 1,25$(OH)_2D_3$ (**1**) complex. (B) 25*S*-Adamantylvitamin D (**4b**) complex. (C) 25*R*-Adamantylvitamin D (**4a**) complex.

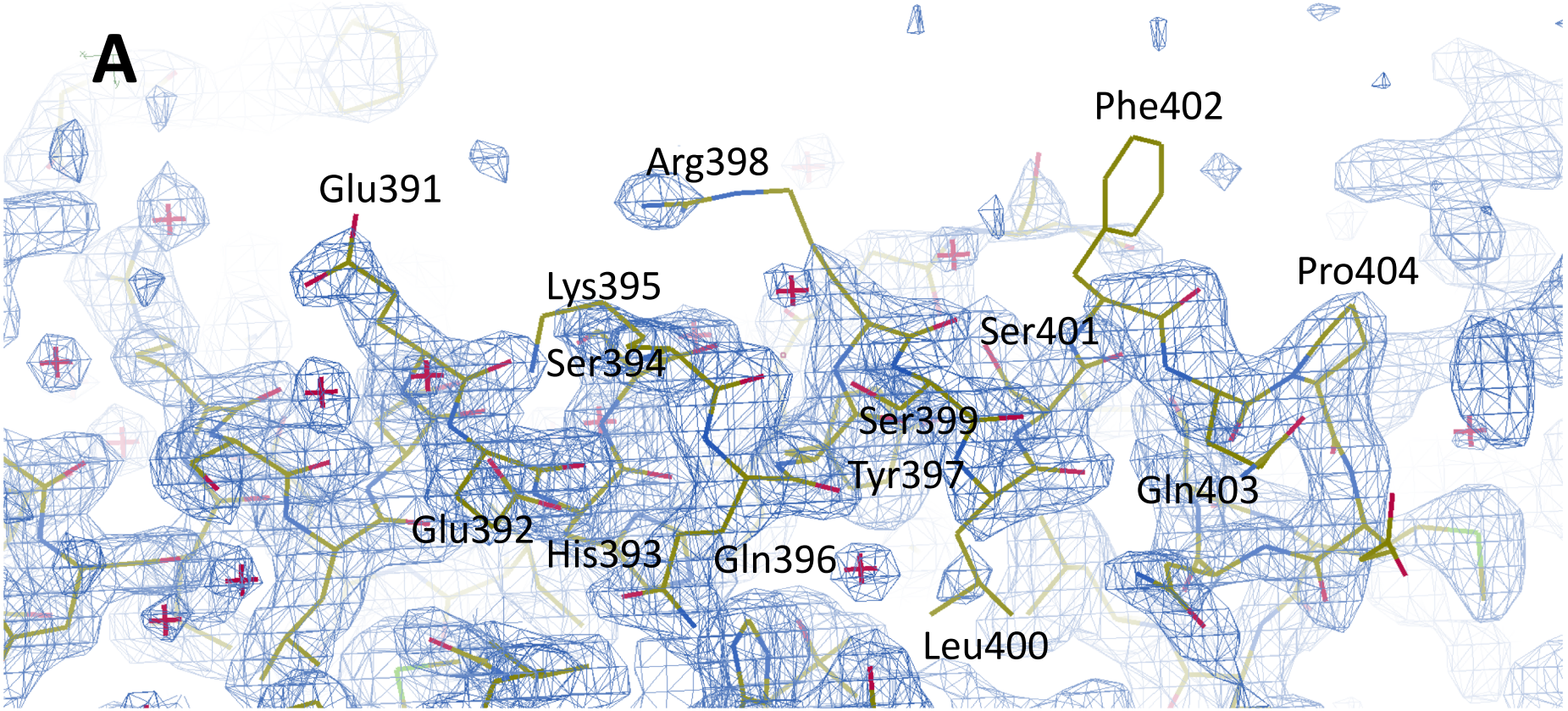

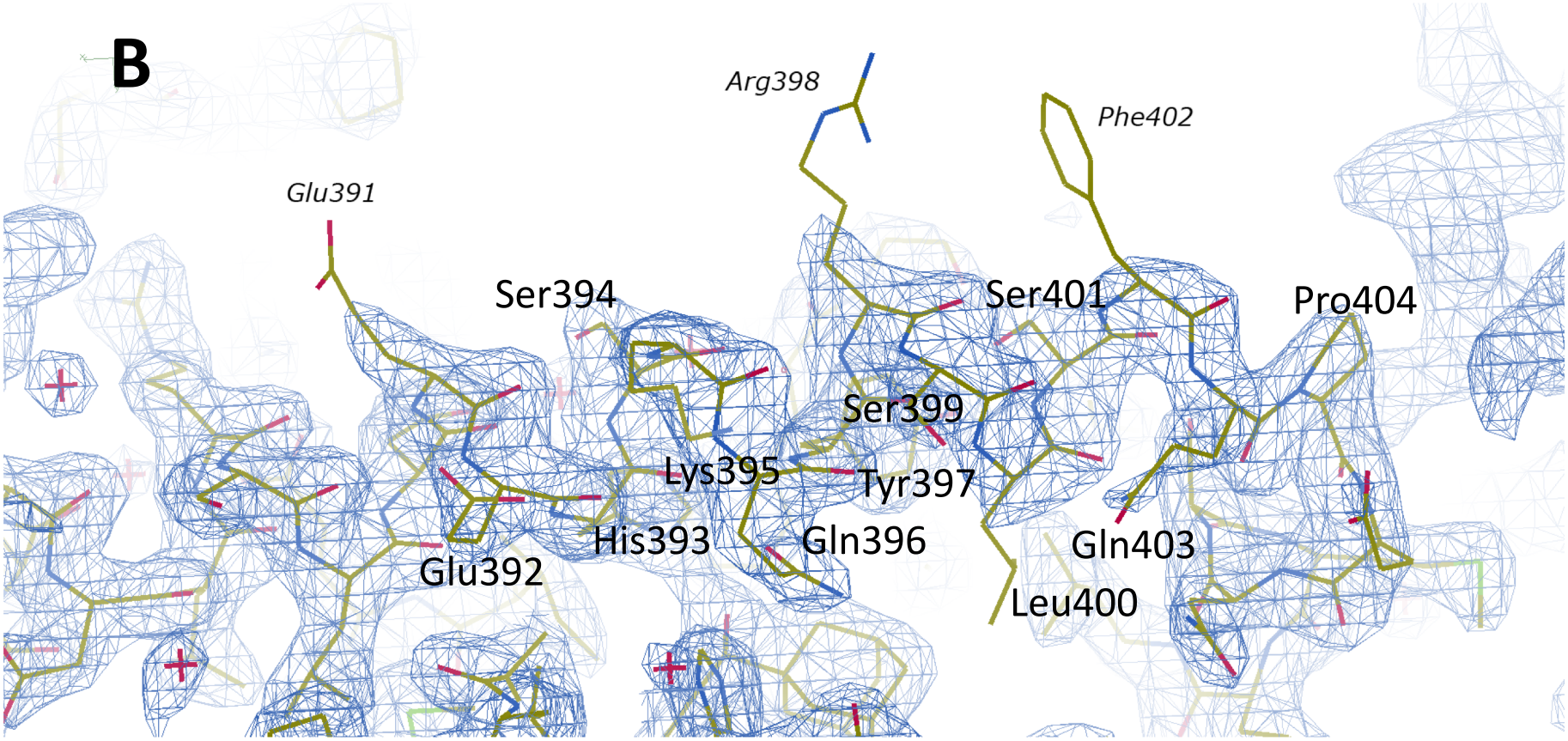
B
Arg398
Phe402
Glu391
Ser394
Ser401
Pro404
Ser399
Lys395
Tyr397
His393
Gln396
Gln403
Glu392
Leu400

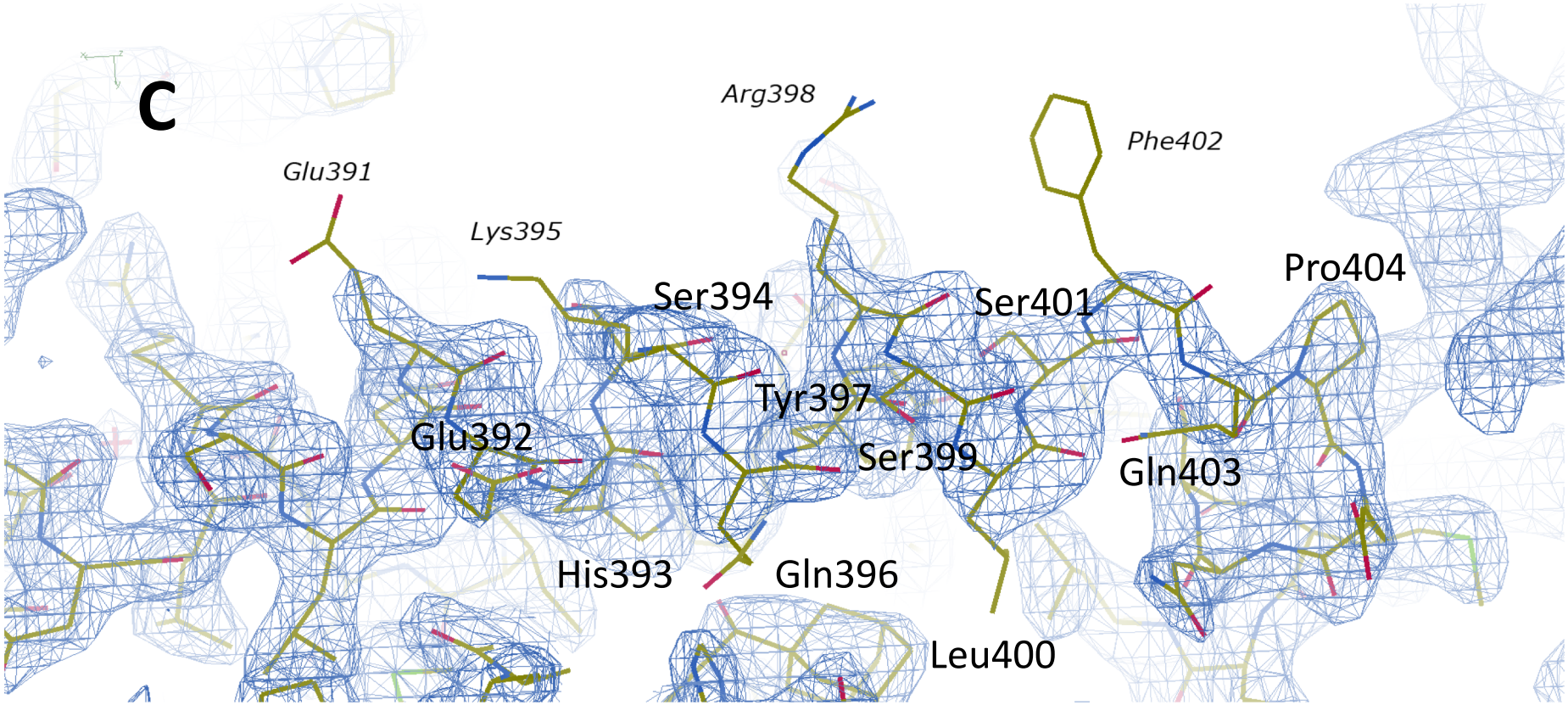
C
Arg398
Phe402
Glu391
Lys395
Ser394
Ser401
Pro404
Tyr397
Glu392
Ser399
Gln403
His393
Gln396
Leu400

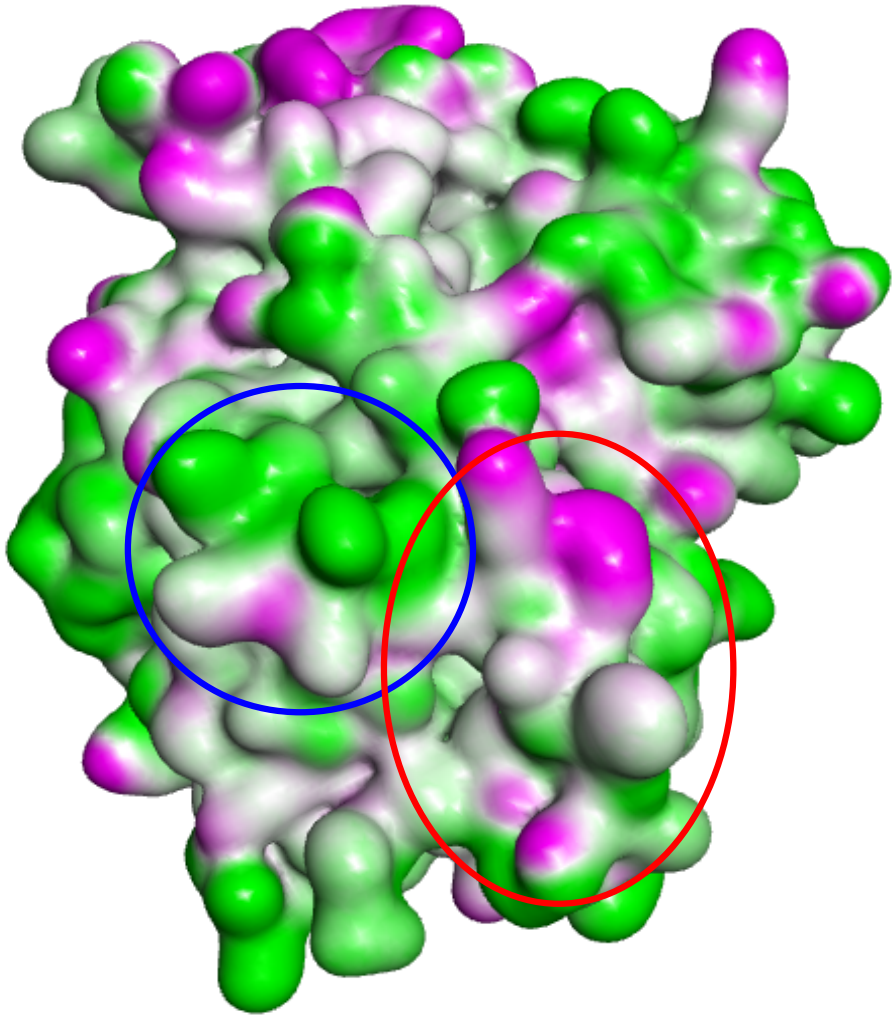

Figure S5. Surface structure of VDR-LBD/19-nor-2-methylene vitamin D derivative (**2b**) complex with hydrogen-bond donor (green)/acceptor (magenta) colors. Helix 11 and 7 regions are circled in red and blue, respectively.

Table S1. Data Collection and Refinement Statistics

*Values in parentheses are for highest-resolution shell.

	4a	4b
Data collection		
Spacegroup	C2	C2
Cell dimensions		
a, b, c (Å)	153.7, 41.8, 42.0	154.1, 41.1, 41.4
b (deg)	95.6	96.4
Resolution (Å)	50-1.99 (2.07-1.99)	50-2.10 (2.22-2.10)
R_{sym}	0.078 (0.607)	0.079 (0.427)
Completeness (%)	98.6 (95.7)	99.1 (99.0)
Redundancy	3.2 (3.2)	3.3 (3.3)
Average I/σ(I)	7.5 (1.4)	9.6 (3.3)
Refinement		
Resolution (Å)	50-2.0	50-2.1
No of reflections	17148	14429
R_{work} / R_{free}	0.194/0.243	0.161/0.214
No of atoms		
protein atoms	2004	1984
ligand atoms	38	38
solvent atoms	12	54
RMS deviations		
bond length (Å)	0.016	0.016
bond angles (deg)	1.90	1.83
Average B-factor (Å²)	50.6	43.5
PDB entry ID	5XZH	5XZF

The ^{1}H and ^{13}C NMR spectra of compounds **4a**, **4b**, **5a**, **5b**, **6**, **8**, **13**, **14**, **15**, **16**, **17**, and **18**.

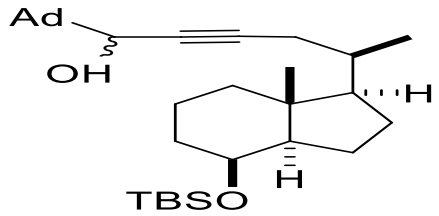

13

^{1}H NMR ($CDCl_3$, 250 MHz)

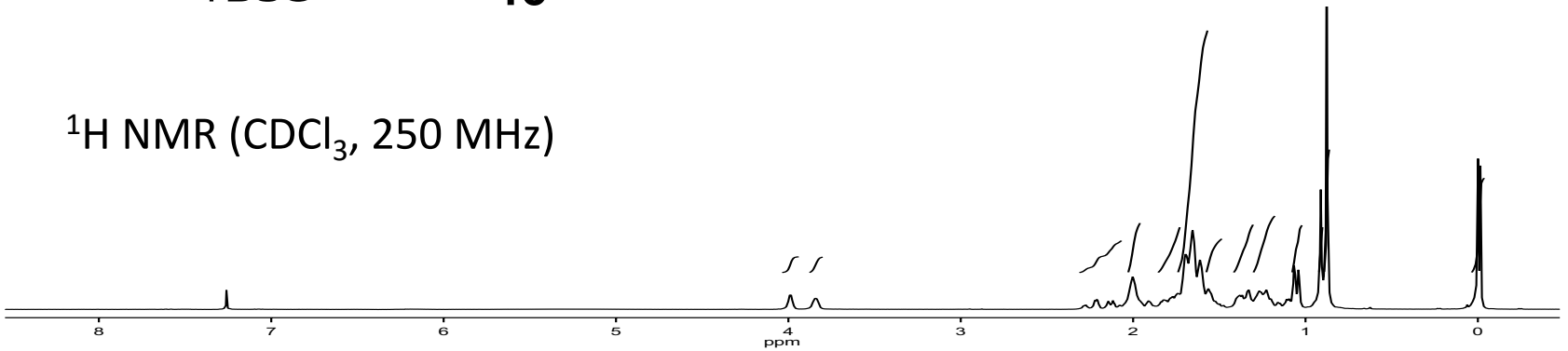

^{13}C NMR ($CDCl_3$, 63 MHz)

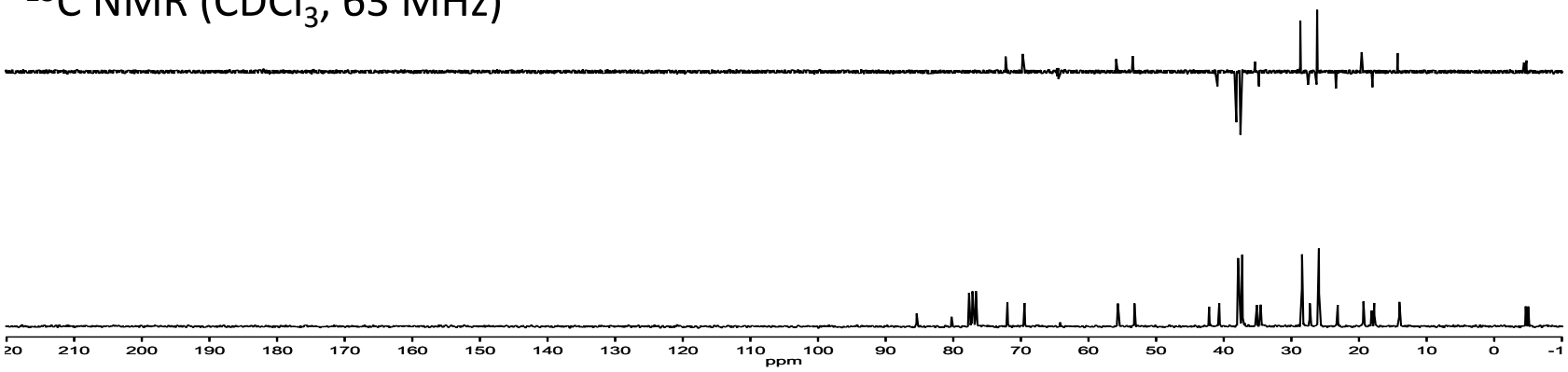

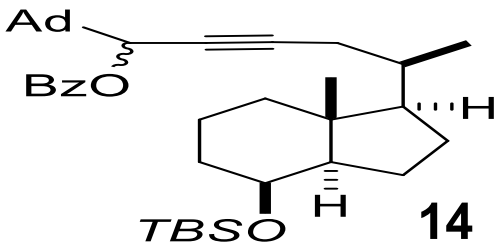

14

^{1}H NMR ($CDCl_3$, 250 MHz)

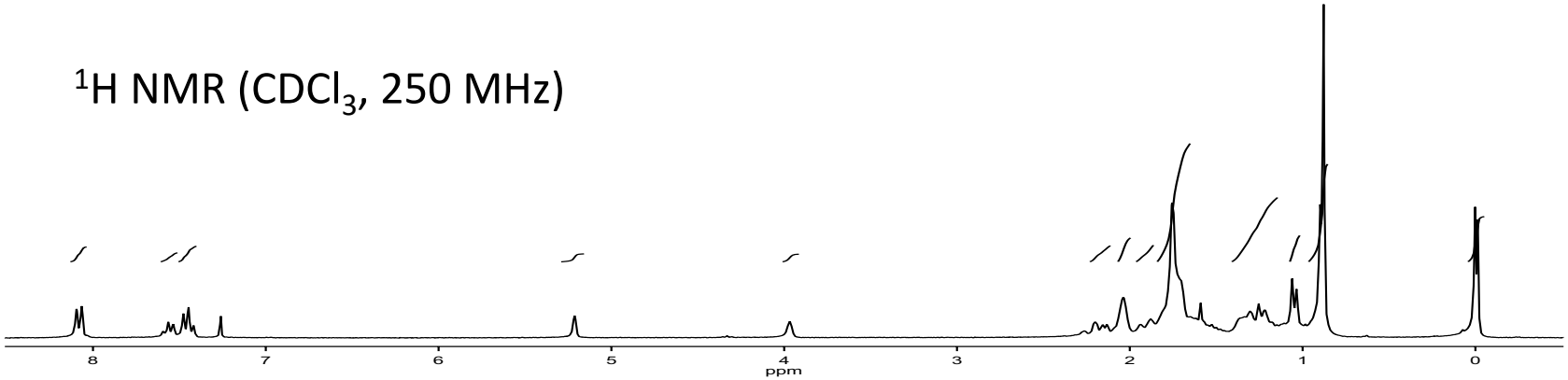

^{13}C NMR ($CDCl_3$, 63 MHz)

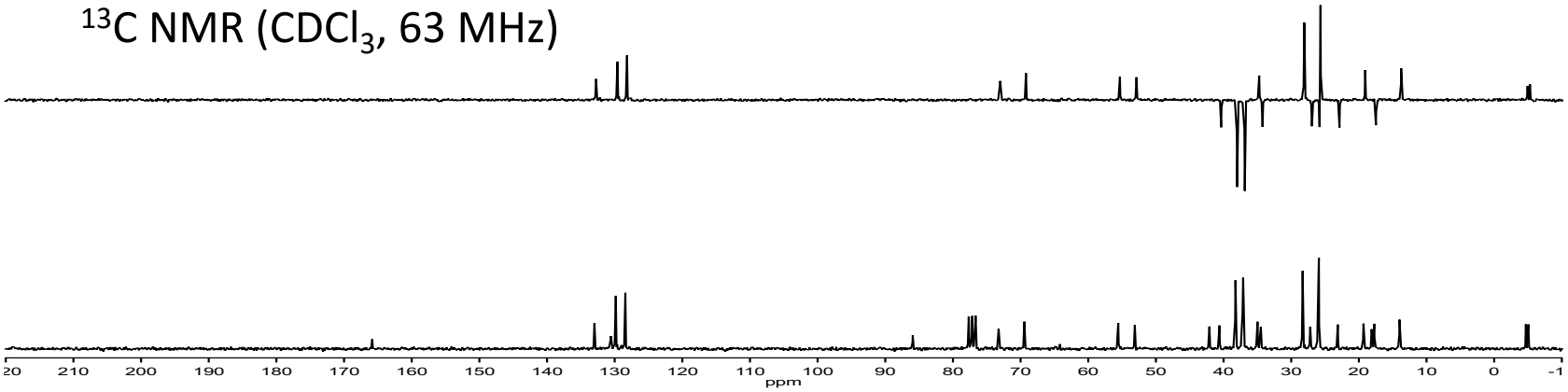

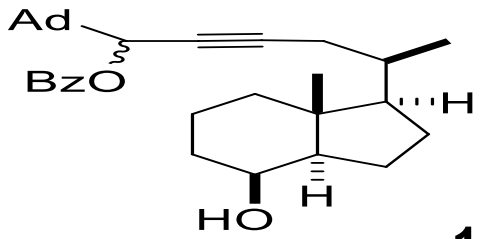

15

^{1}H NMR ($CDCl_3$, 250 MHz)

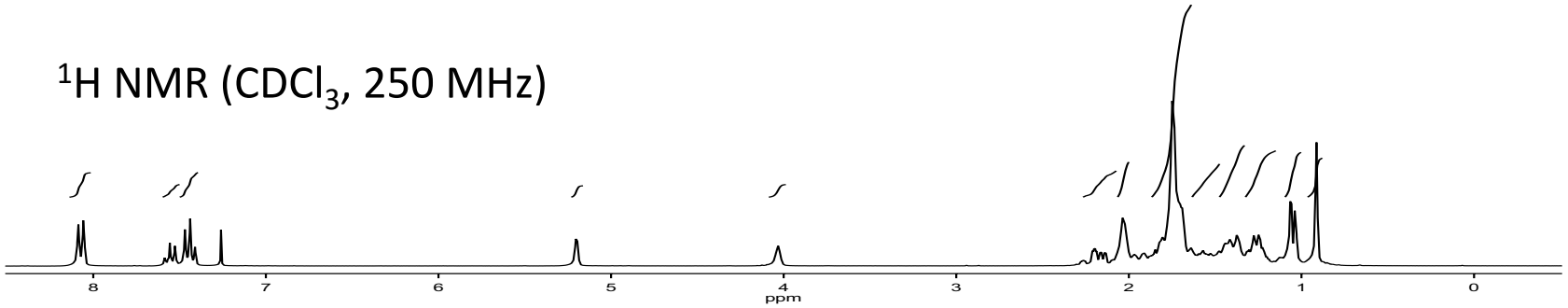

^{13}C NMR ($CDCl_3$, 63 MHz)

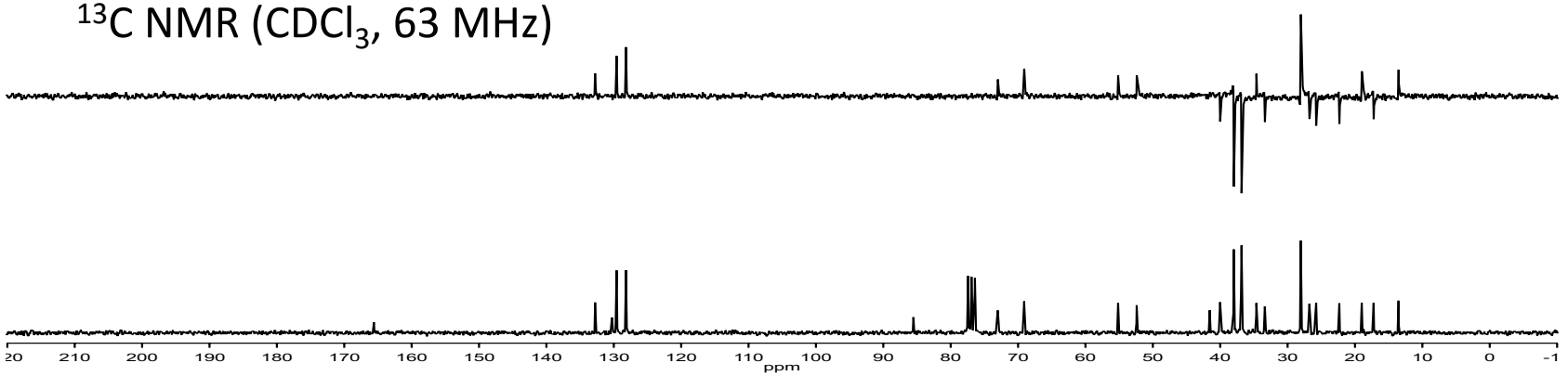

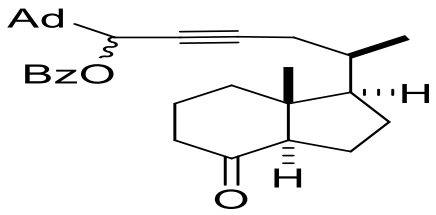

16

^{1}H NMR ($CDCl_3$, 250 MHz)

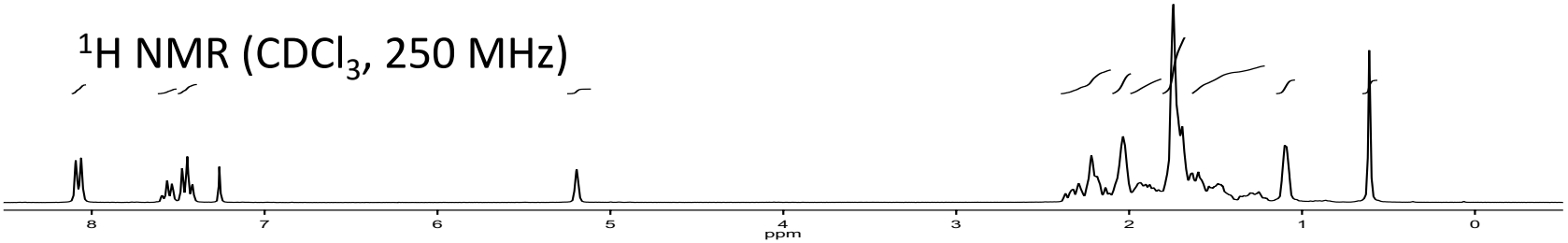

^{13}C NMR ($CDCl_3$, 63MHz)

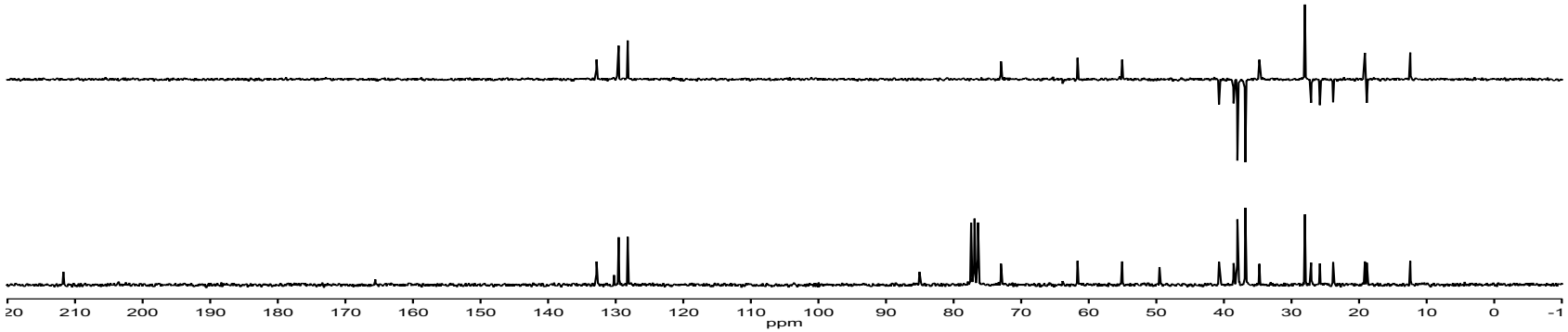

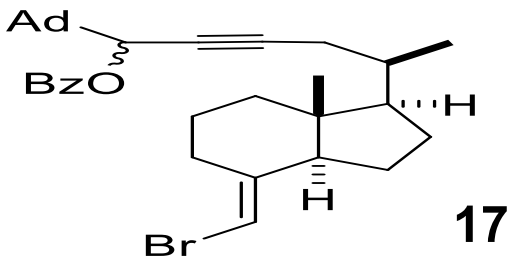

17

^{1}H NMR ($CDCl_3$, 250 MHz)

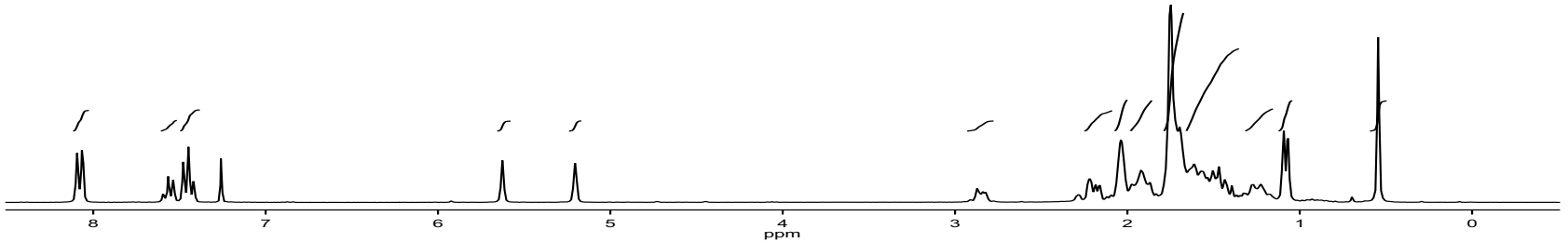

^{13}C NMR ($CDCl_3$, 63MHz)

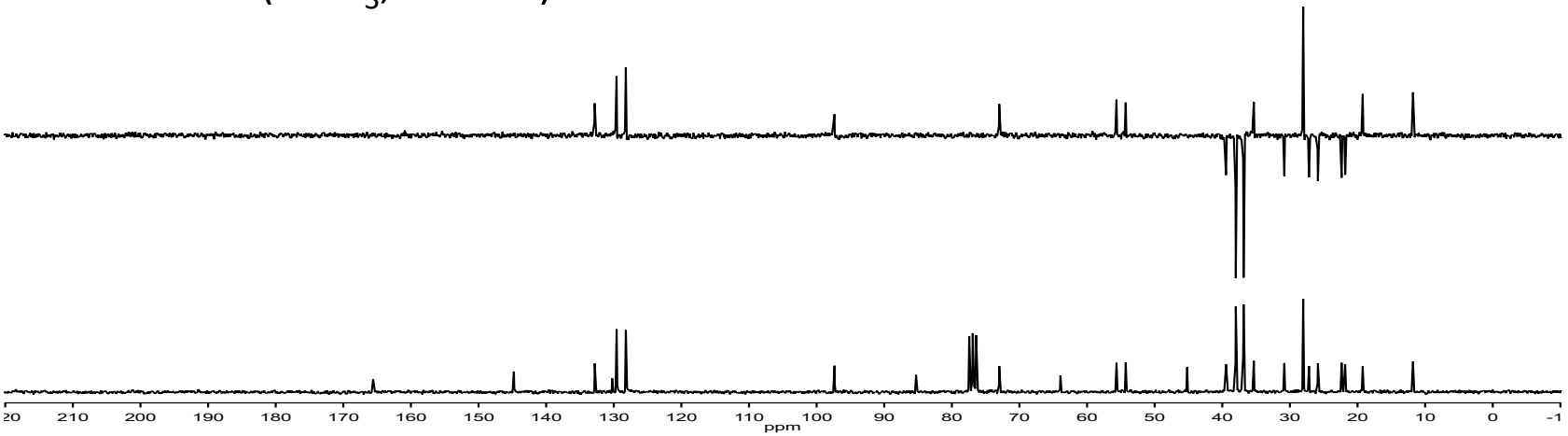

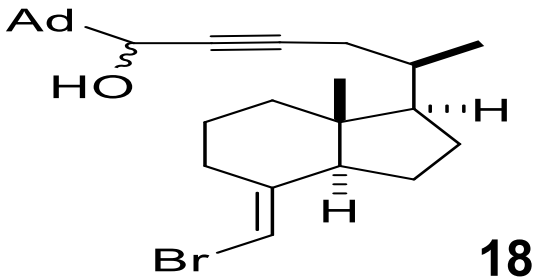

18

^{1}H NMR ($CDCl_3$, 250 MHz)

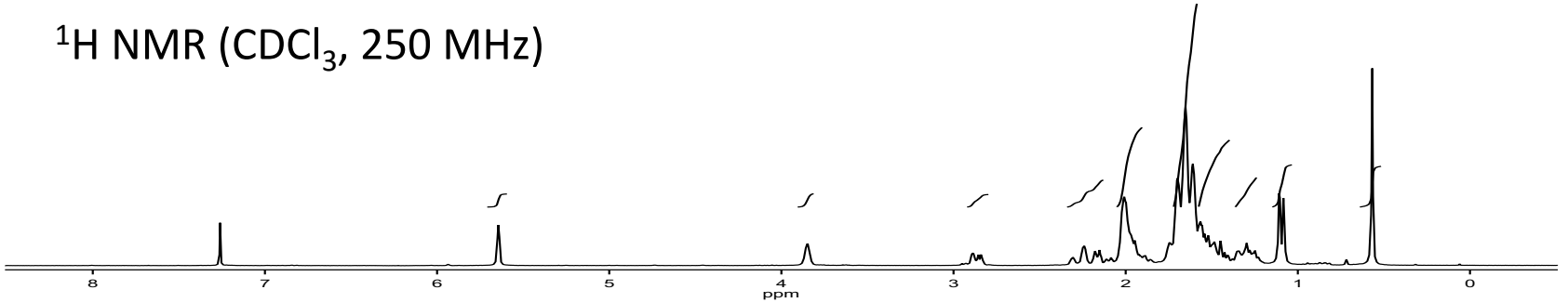

^{13}C NMR ($CDCl_3$, 63MHz)

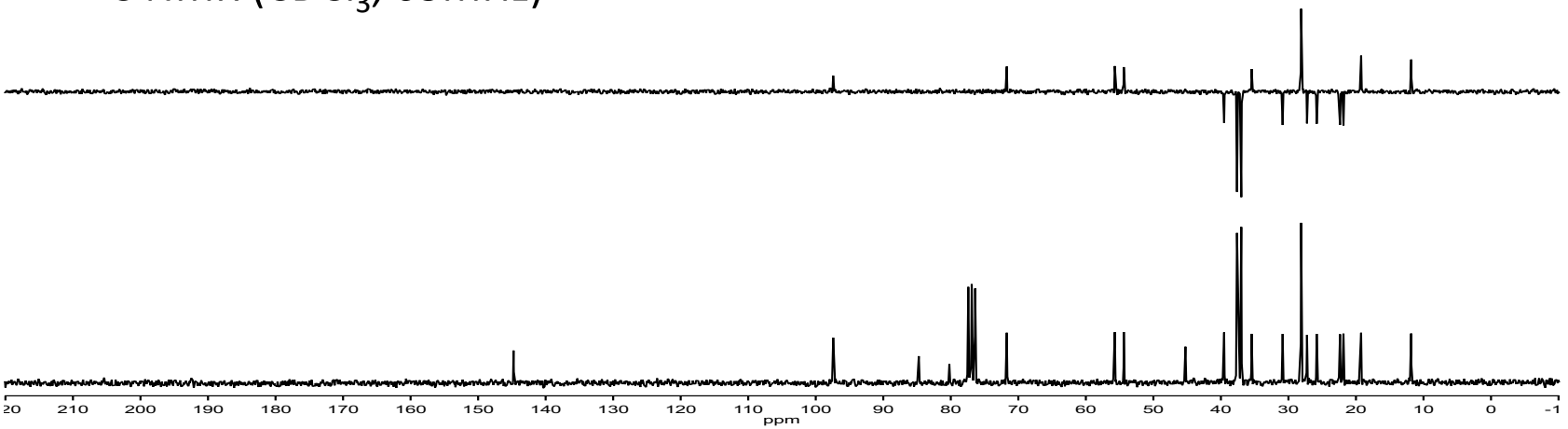

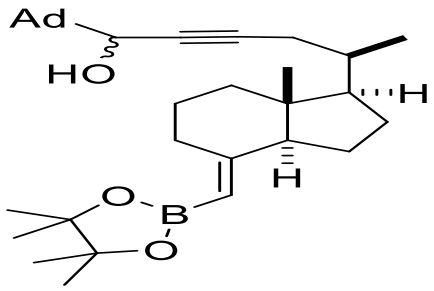

8

^{1}H NMR ($CDCl_3$, 250 MHz)

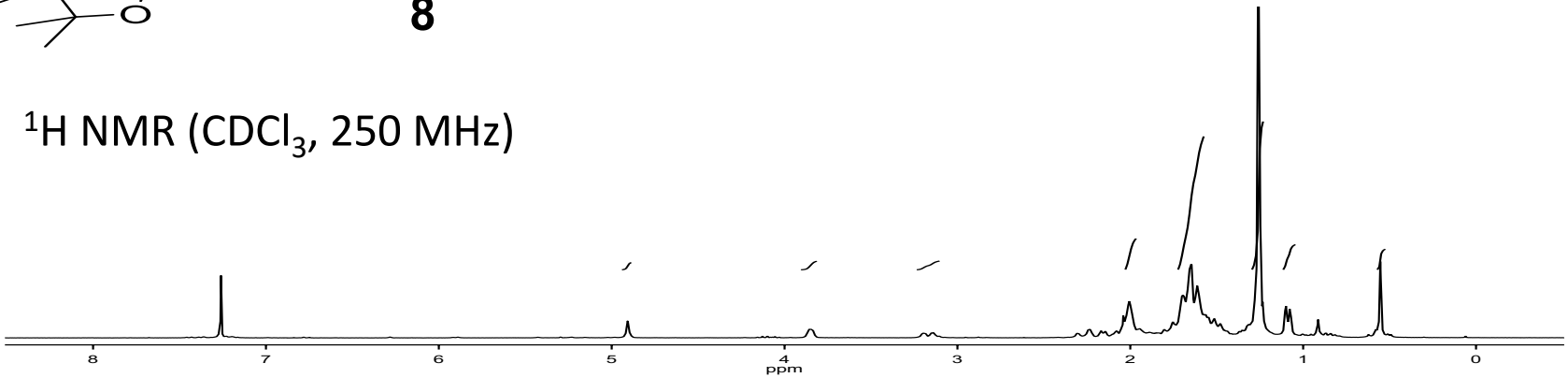

^{13}C NMR ($CDCl_3$, 63MHz)

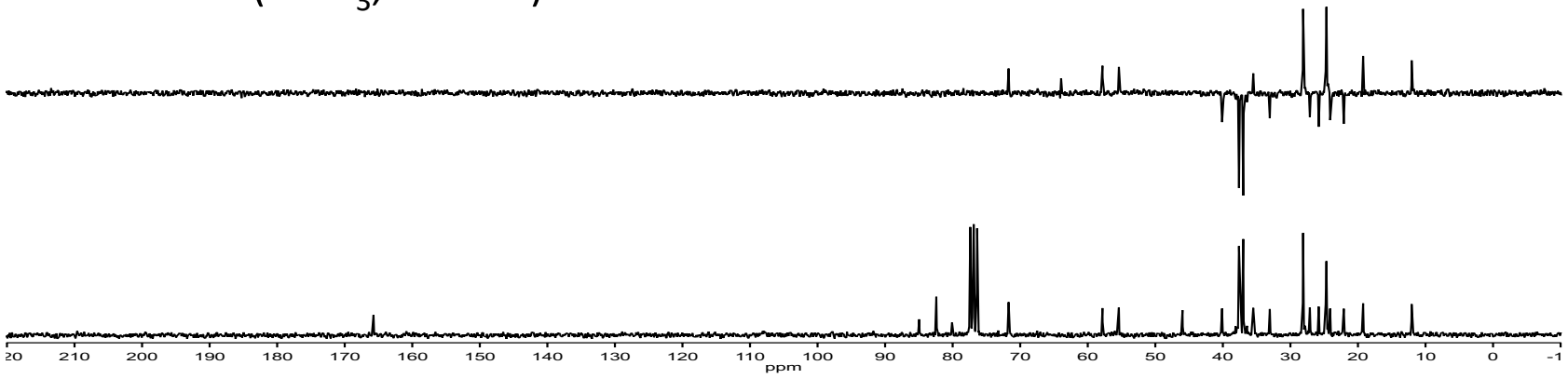

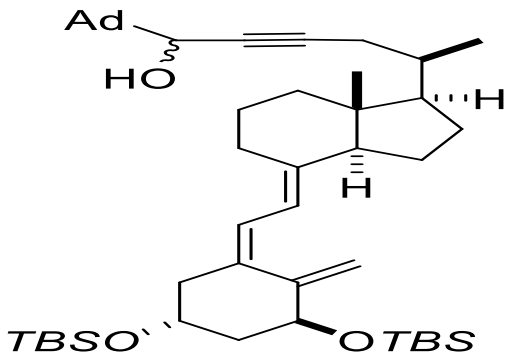

6

^{1}H NMR ($CDCl_3$, 250 MHz)

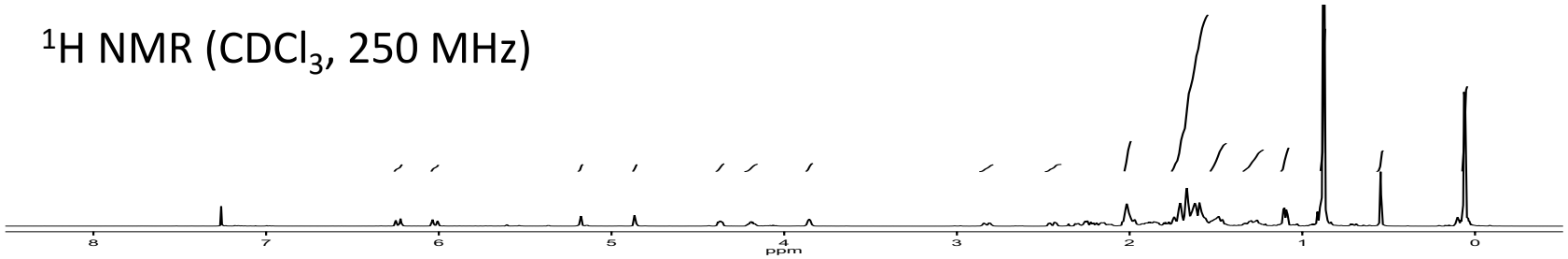

^{13}C NMR ($CDCl_3$, 63MHz)

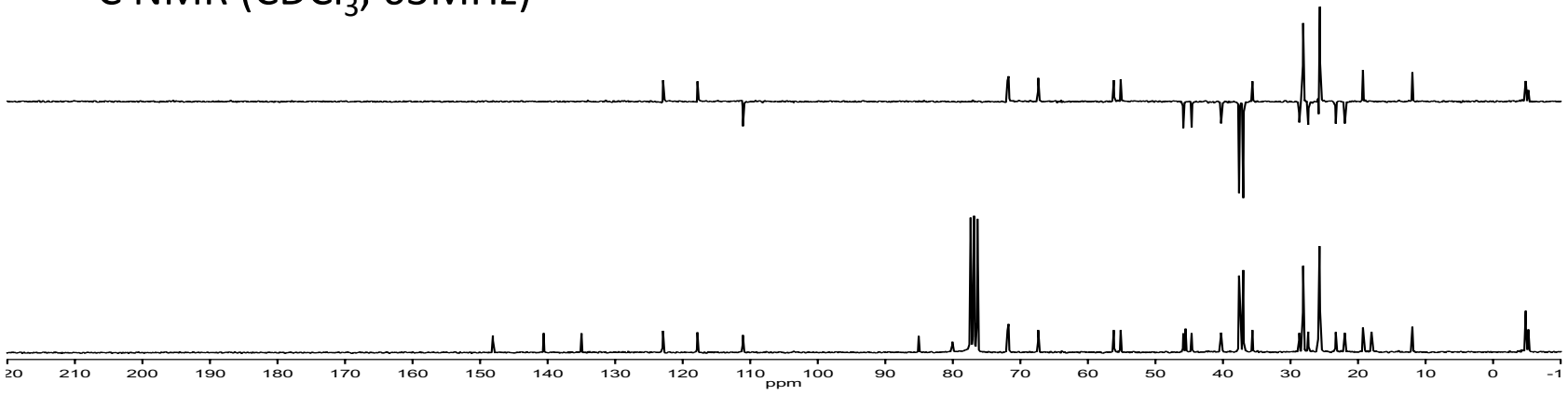

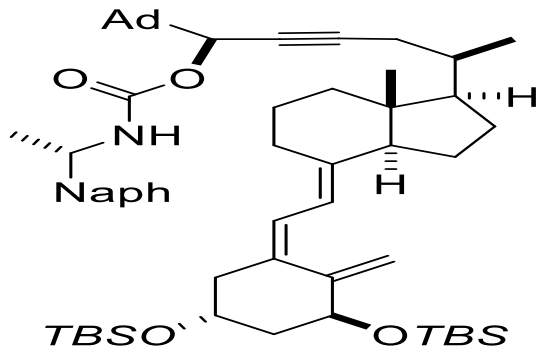

5b

^{1}H NMR ($CDCl_3$, 250 MHz)

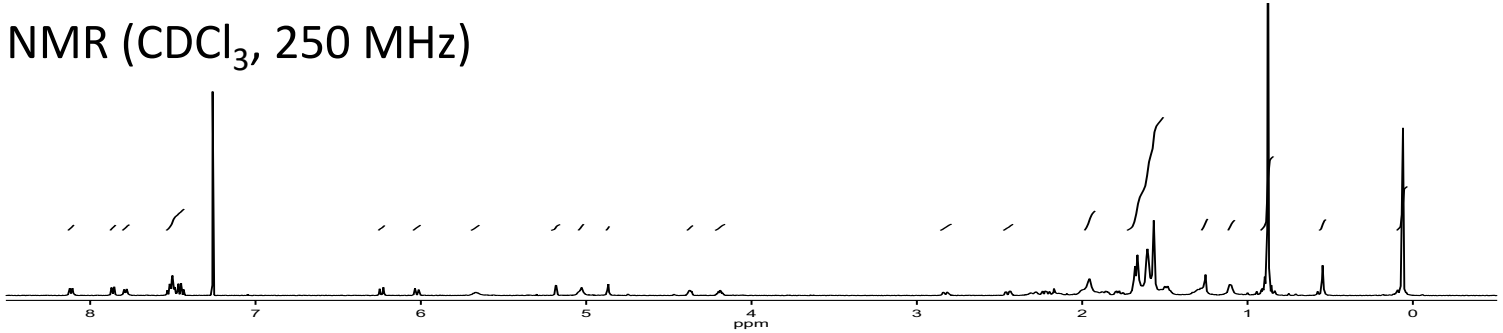

^{13}C NMR ($CDCl_3$, 63MHz)

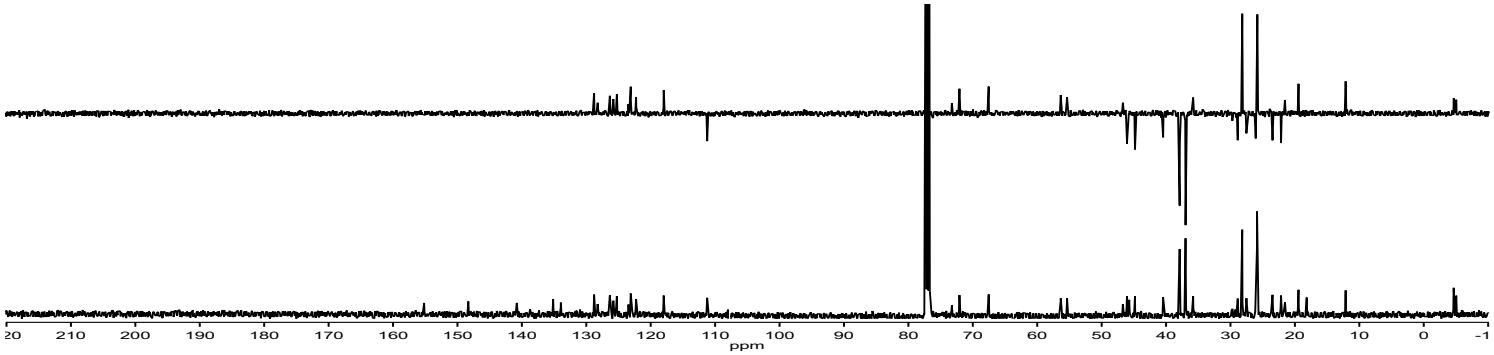

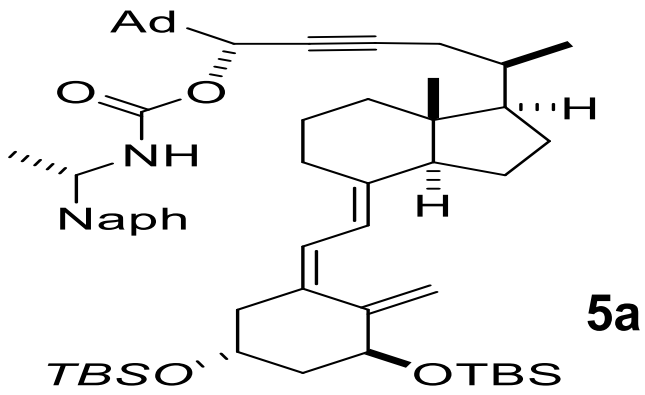

5a

^{1}H NMR ($CDCl_3$, 250 MHz)

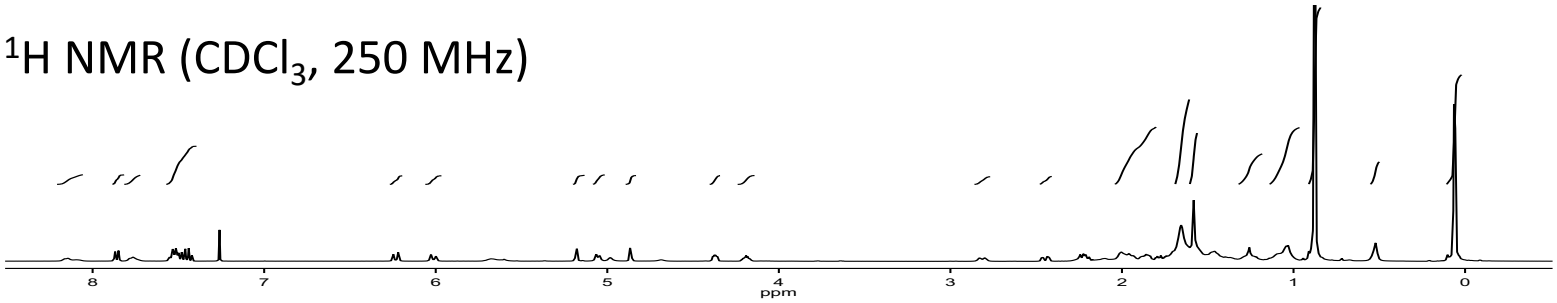

^{13}C NMR ($CDCl_3$, 63MHz)

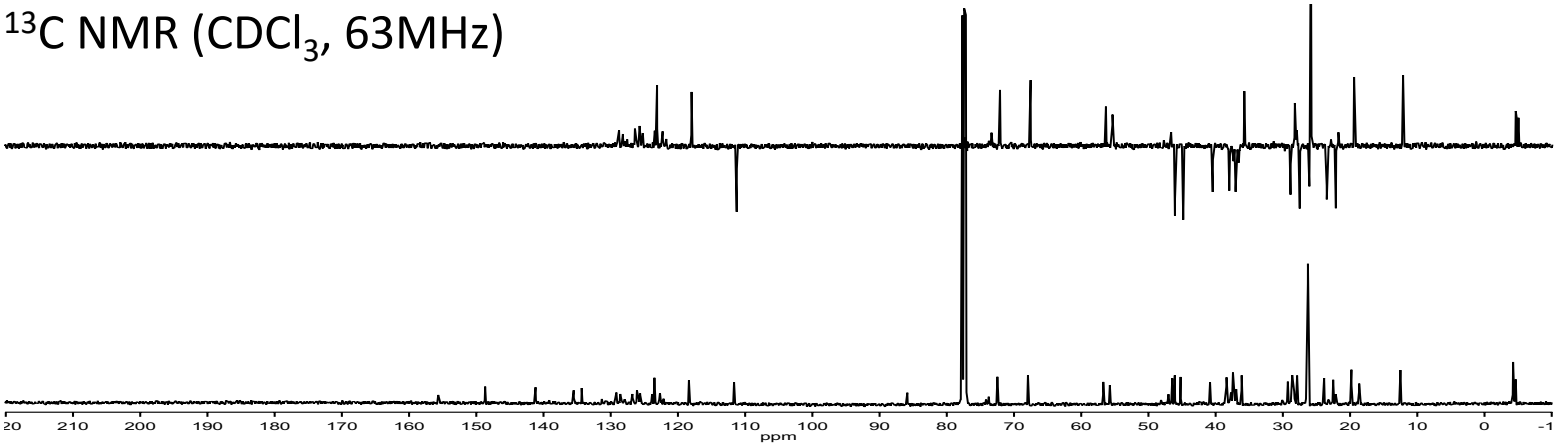

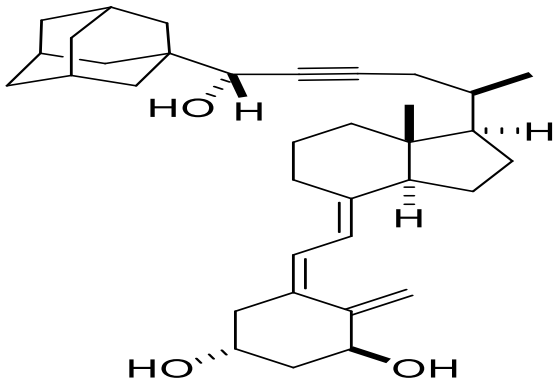

4a

^{1}H NMR ($CDCl_3$, 250 MHz)

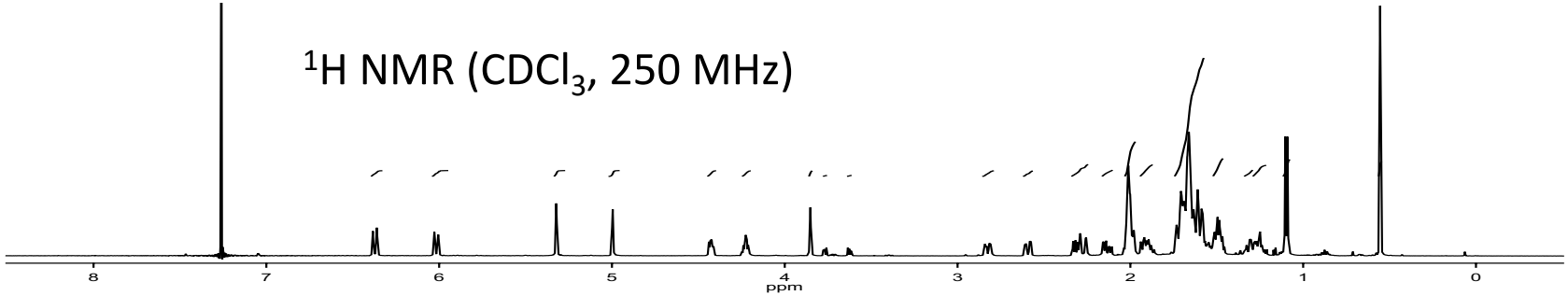

^{13}C NMR ($CDCl_3$, 63MHz)

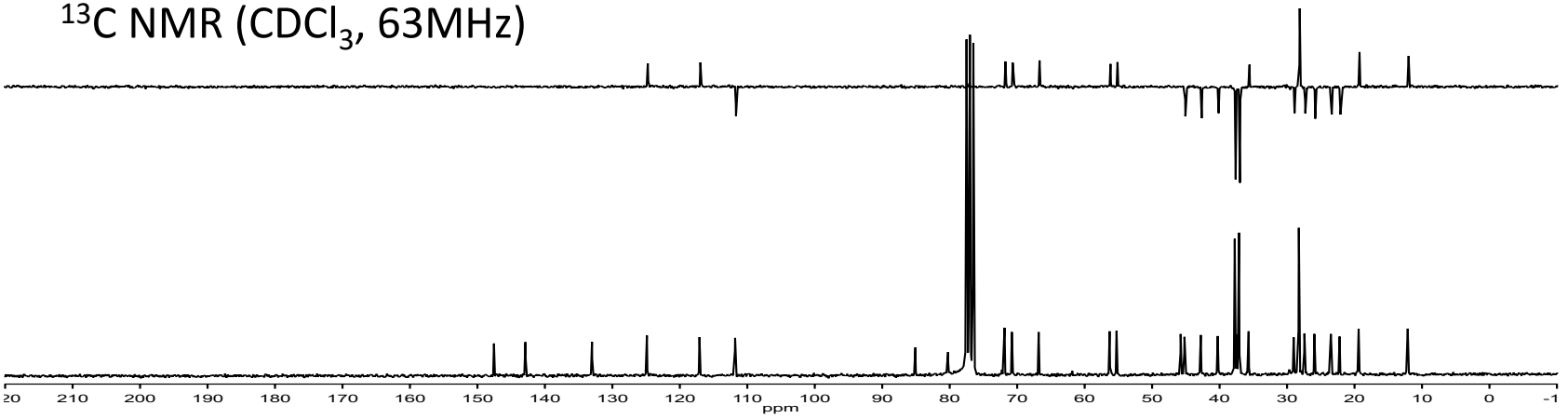

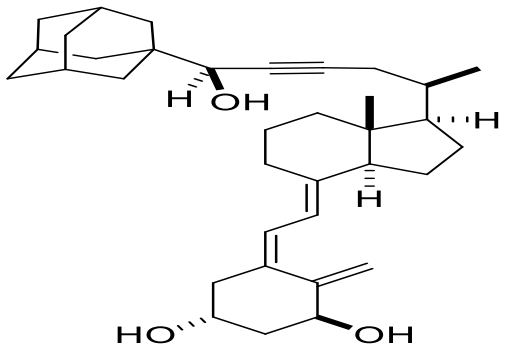

4b

^{1}H NMR ($CDCl_3$, 250 MHz)

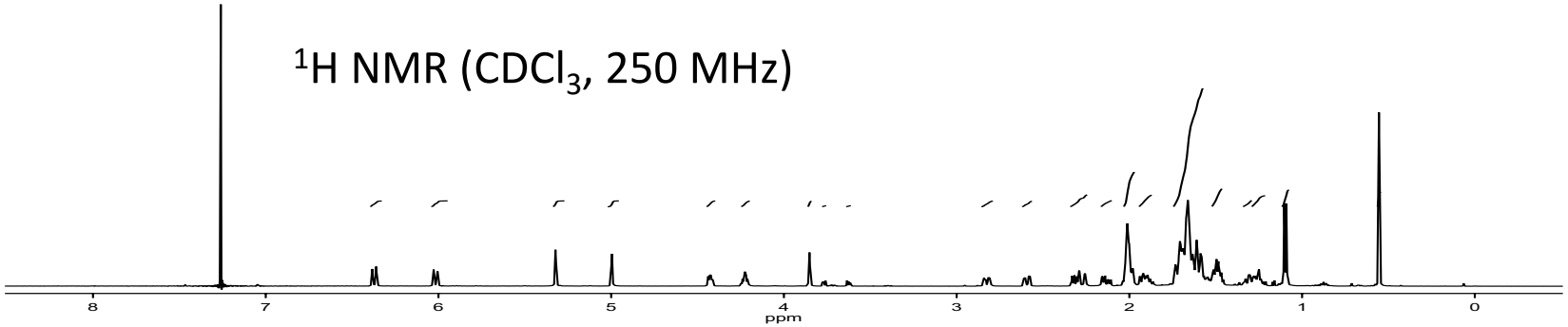

^{13}C NMR ($CDCl_3$, 63MHz)